Formation and Microscopic Investigation of Iron Oxide Aligned Nanowires Into Polymeric Nanocomposite Films

DESPINA FRAGOULI,[1]* BRUNO TORRE,[2] GIOVANNI BERTONI,[2] RAFFAELLA BUONSANTI,[3] ROBERTO CINGOLANI,[1,2] AND ATHANASSIA ATHANASSIOU[1,3]
[1]*Center for Bio-Molecular Nanotechnologies,CBN, of IIT@UniLe, via Barsanti c/o STAMMS, Arnesano 73010, (LE) Italy*
[2]*Italian Institute of Technology, IIT, via Morego 30, 16152 Genova, Italy*
[3]*National Nanotechnology Laboratory, NNL, of CNR-INFM, Università del Salento, via per Arnesano km 5, 73100 Lecce, Italy*

KEY WORDS colloidal nanocrystals; polymers; magnetic assembly; magnetic force microscopy

ABSTRACT We present a microscopic investigation of nanocomposite films of iron oxide (γ-Fe_2O_3) magnetic nanowires (NWs) aligned into polymers, formed upon evaporation of solutions of acrylate polymer/magnetic nanoparticles under magnetic field (MF). The field causes the assembly of the γ-Fe_2O_3 nanoparticles along the direction of the MF lines, resulting in magnetic NWs embedded throughout the entire volume of the polymer film. The scanning electron microscopy and the transmission electron microscopy studies show that the cylindrical-shaped NWs have $\sim$15-μm average length and are isotropically distributed throughout the film. The study with the MF microscopy technique not only proves that the composed NWs are magnetic but also makes possible the magnetic study of each individual NW in a nondestructive way. In this way it becomes possible for the localized study of the magnetic properties alteration after the binding of various molecules onto individual NWs, opening up the way of using these films in sensor devices applied in various fields ranging from biology to environmental purposes. *Microsc. Res. Tech. 73:952–958, 2010.*

INTRODUCTION

The magnetic nanoparticles have generated much interest nowadays because of their unique properties (e.g., chemical resistance, biocompatibility, electromagnetic properties, and hardness) that are essential in a large range of applications in fields such as biology, magnetic sensors, and microfluidics. For many of these applications, the ordering of the nanoparticles into high density and spatially oriented arrays of nanowires (NWs) is critical, due to the novel collective properties of the latter, evidently different from those of isolated nanoparticles (Tang and Kotov, 2005). For the magnetic NWs formation, various techniques have been developed, such as the molecularly linked induced assembly under or not magnetic fields (MFs) (Goubalt et al., 2005; Singh et al., 2005), templating techniques using polymer–nanoparticles mixtures (Martin and Mijangos, 2009), or the use of controllable external MFs (Lallatone et al., 2004; Park et al., 2007; Sahoo et al., 2004) during evaporation of nanoparticles/solvent solutions. Especially, the latter technique is an attractive option for the fabrication of 1D magnetic NWs, due to its extreme simplicity, effectiveness, and speed.

In parallel, the incorporation of nanoparticles or nanofibers in polymers also attracts particular research attention because of the synergistic and hybrid properties derived from the individual components (Schmidt and Malwitz, 2003). Specifically, the fabrication of nanocomposites consisting of aligned NWs in polymer matrices results into novel materials with anisotropically enhanced physical properties, combining the intrinsic properties of the polymers with the highly anisotropic properties of the aligned units (Jestin et al., 2008; Kimura et al., 2002), ready to be used in various polymer-based technological applications. In particular, the magnetic NWs-based nanocomposites have great potentiality in information storage (Weller and Doerner, 2000), sensing (Kaushik et al., 2009), actuation (Fahrni et al., 2009), molecular separation (Merkel et al., 2002), and electromagnetic wave absorption (Huo et al., 2009). The use of strong MF ($\sim$10 T) for the alignment of the fillers in the polymers has been used in the past mostly in the field of the carbon nanotube composites where the tubes are oriented in the matrix during the curing of the polymer or during the evaporation of the solvent (Kimura et al., 2002). Very few studies have used MFs for the orientation of nanoparticles, in order to form NWs in polymers. This technique has been applied mainly on particles of micrometer sizes (Martin et al., 2000). The dispersion of magnetic nanoparticles in polymer/prepolymer solutions and the subsequent orientation during evaporation/curing under weak MFs resulted only to the formation of oriented aggregates (Fahrni et al., 2009; Jestin et al., 2008).

In this work, we present the simultaneous topographic and magnetic study of 1D magnetic NWs, formed by the assembly of iron oxide (γ-Fe_2O_3) colloidal nanoparticles in polymer matrices under the application of MF. The formation of the NWs is done in situ, during the drying of a casted polymer solution mixed with γ-Fe_2O_3 nanoparticles, in a weak homogeneous MF (160 mT). The microscopic investigation of the

*Correspondence to: Despina Fragouli, Center for Bio-Molecular Nanotechnologies, CBN, of IIT@UniLe, via Barsanti c/o STAMMS, Arnesano 73010, (LE) Italy. E-mail: despina.fragouli@iit.it

Received 11 January 2010; accepted in revised form 30 January 2010
DOI 10.1002/jemt.20848
Published online 15 March 2010 in Wiley Online Library (wileyonlinelibrary.com).

topography and of the magnetic properties of the film is done with magnetic force microscopy (MFM) showing that the external MF causes the nanoparticles assembly toward its direction, resulting in magnetic NWs. A localized magnetic study of each NW was performed in a nondestructive way, opening up the possibility of studying the magnetic response after binding such stripes with various molecules. Moreover, the formed NWs are studied by transmission electron microscopy (TEM) and scanning electron microscopy (SEM), where it is confirmed that the NWs are aligned in the entire film volume, have cylindrical shape, and average length $\sim$15 μm.

MATERIALS AND METHODS

Samples Preparation

The γ-Fe_2O_3 colloidal nanocrystal spheres of 10-nm diameter were synthesized by modifying a wet-chemical synthetic approach reported by Sun et al. (2004). $Fe(CO)_5$ was used as the precursor, whereas oleic acid, oleylamine, and hexadecane-1,2-diol were used as both reactants and capping molecules.

One millimolar solution of the copolymer poly(ethylmethacrylate-*co*-methylacrylate) (PEMMA) in chloroform was prepared by dissolving 100 mg of PEMMA per 1 mL of solvent. For the preparation of the solution of 1% wt γ-Fe_2O_3 nanoparticles and 99% wt PEMMA, 15 μL of 0.4 M γ-Fe_2O_3/chloroform solution was added in 1 mL of the PEMMA solution. After sonication for 10 min, to avoid the formation of aggregates, the resulting solution was drop-casted on a carefully cleaned glass substrate and left to dry overnight under saturated chloroform atmosphere. For the alignment of the nanoparticles, the system was subjected to a homogeneous MF ($\sim$160 mT), produced by two permanent magnets, applied parallel to the substrate during the deposition and evaporation process.

Samples Characterization

The films were initially studied under an optical microscope (Olympus BX41). More detailed analysis was obtained with a SEM (JEOL JSM-6490LA) detecting the backscattered electrons (BSE), and a 100 kV TEM (JEOL JEM-1011) in bright field mode, imaging thin film sections, which were cut with a Leica EM UC6 Ultramicrotome. The NWs average length and diameter were measured from SEM and TEM images, averaging at least 30 wires.

Sample morphology and magnetic data are acquired by means of MFP-3D atomic force microscope (Asylum Research, Santa Barbara CA) using MFM technique to resolve magnetic structure with nanometer resolution. Magnetic forces are detected using noncontact cantilevers covered with a thin magnetic film on the tip sides to enhance specific sensitivity, and signal is detected in a modified dynamic-AFM mode allowing to separate (long range) magnetic forces from (short range) topography ones.

The technique operates in two steps. First, a single line of a topography map is acquired in amplitude modulation mode and stored. In this mode, the tip is in intermittent contact with the surface, whereas the damping in the free oscillation amplitude is used to adjust tip-sample distance [slope detection technique (Marti et al., 1987)]. In this step, the dominating contribution to average force is repulsion, giving the topography of the sample.

As a second step, the same line is repeated, whereas the tip is lifted at a Δz distance from the surface, which is calculated from the height data measured in previous step. This mode (called NAP) is remarkably different from commonly used constant height technique, because surface tilt and roughness are point-by-point compensated using the previously obtained topography data. In this way, the contribution of short-range forces is held constant, whereas the long-range forces (at a known Δz distance) are probed by monitoring oscillation parameters of the cantilever. Usually, the changes in free oscillation frequency are considered a good estimation of long-range forces, because in a single harmonic oscillator model of the cantilever, these quantities are related as follows:

$$\Delta f = \frac{1}{2\pi}\sqrt{\frac{\left(k_0 - \frac{dF(z)}{dz}\right)}{m}} - f_0 \qquad (1)$$

where m_0, k_0, and f_0 are mass, spring constant, and free oscillation amplitude of the oscillator (depending therefore on the sensor), and Δf is a frequency variation induced by force changes. On a compositionally homogeneous sample with different magnetic domains (uniform short-range forces and different long-range ones), the frequency signal in NAP mode would provide a direct contrast of force variation at constant distance from the surface, that is, magnetic features.

To measure the representative parameters of our films, the right choice of the cantilever is essential. A proper choice of cantilever properties, as magnetic and mechanical ones, deeply influences lateral resolution and sensitivity and defines the best NAP height from the surface. This height has to be selected to minimize the short-range repulsive (topography) interaction. Eventually, the recorded images result by an appropriate compromise between crosstalk, sensitivity, and lateral resolution. In our samples, the influencing parameters can be the nanoparticle aggregation, the features shape, and the distance from the surface. Therefore, many critical factors such as mechanical properties in short-range regime or tip-particle distance for long-range forces have a wide variability. Moreover, the used γ-Fe_2O_3 nanoparticles of 10-nm diameter are expected to have paramagnetic behavior, giving a quite small magnetic response with respect to bulk domains. To perform cantilever selection, a test sample has been prepared as follows: a 0.4-M γ-Fe_2O_3/chloroform solution has been further diluted in its solvent by a factor 10^4 and drop casted on a freshly cleaved highly ordered pyrolytic glaphite (ZYB Quality, NT-MDT, Moscow) to allow isolated particle groups with single-layer thickness on an atomically flat substrate. Comparative MFM measurements at different Δz distances (data not shown) lead us to select Nanosensors PPP-MFMR cantilevers with the following nominal parameters:

- Hard magnetic coating on the tip side (coercivity of $\sim$300 Oe, remanence magnetization of $\sim$300 emu/cm^3);
- Effective magnetic moment in the order of 10^{-13} emu;

- Guaranteed tip radius of curvature <50 nm;
- Magnetic resolution better than 50 nm;
- Spring constant (3 nN/nm).

With this sensors, the best resolution have been obtained at 30 nm with a free amplitude oscillation of 50 nm. These parameters have been taken as reference and slightly adjusted on different samples.

RESULTS

Chloroform solutions of 1% wt γ-Fe_2O_3 nanoparticles and 99% wt PEMMA were drop casted on glass substrates. For some films, a homogeneous MF (~160 mT), produced by two permanent magnets, was applied parallel to their substrate during the deposition and evaporation process (Fig. 1). All the films were left to dry overnight at saturated chloroform atmosphere under or not MF.

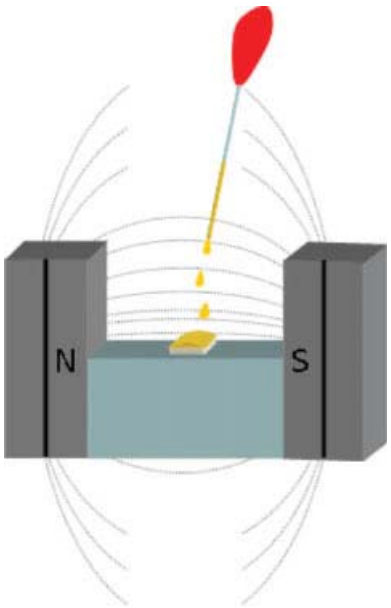

Fig. 1. Experimental set up for the preparation of nanocomposites incorporating magnetic NWs formed under the application of a magnetic field. [Color figure can be viewed in the online issue, which is available at wileyonlinelibrary.com.]

The resulting nanocomposite films were initially studied under an optical microscope to confirm the formation of the magnetic NWs in the case of MF application. Figures 2a and 2b demonstrate the optical microscope images of two films, produced after drop casting and evaporation of the polymer–nanoparticle solution under or not MF, respectively. It is clear that the application of a MF during the deposition of the solution and the evaporation process causes the movement of the nanoparticles toward the direction of the magnetic lines, forming NWs (Fig. 2a). In contrast, when the deposition is done without the presence of the MF, the formed films contain only aggregated structures randomly distributed in the entire volume of the films (Fig. 2b).

The topography study of the films, which was conducted by the MFM (at the NAP mode with the tip lifted about 5 nm from the surface of the films), reveals further microscopic features. The film of 1% wt γ-Fe_2O_3 nanoparticles in PEMMA, which was left to dry without external MF, presents on its surface-aggregated structures with spherical shape of few tens nanometers diameter (Fig. 3a). Figure 3b illustrates the corresponding magnetic image, where it is shown that these aggregates do not have a significantly different magnetic behavior compared to the background matrix. This indicates that these structures are mainly covered by the polymer, which apparently reduces the strength of their magnetic characteristics. Furthermore, the film of 1% wt γ-Fe_2O_3 nanoparticles in PEMMA formed under MF has similar homogeneous surface characteristics. The magnetic NWs that, as the optical microscopy analysis has revealed, are formed in the volume of the film hardly appear on the surface. A surface area of the film, where a NW is present, can be

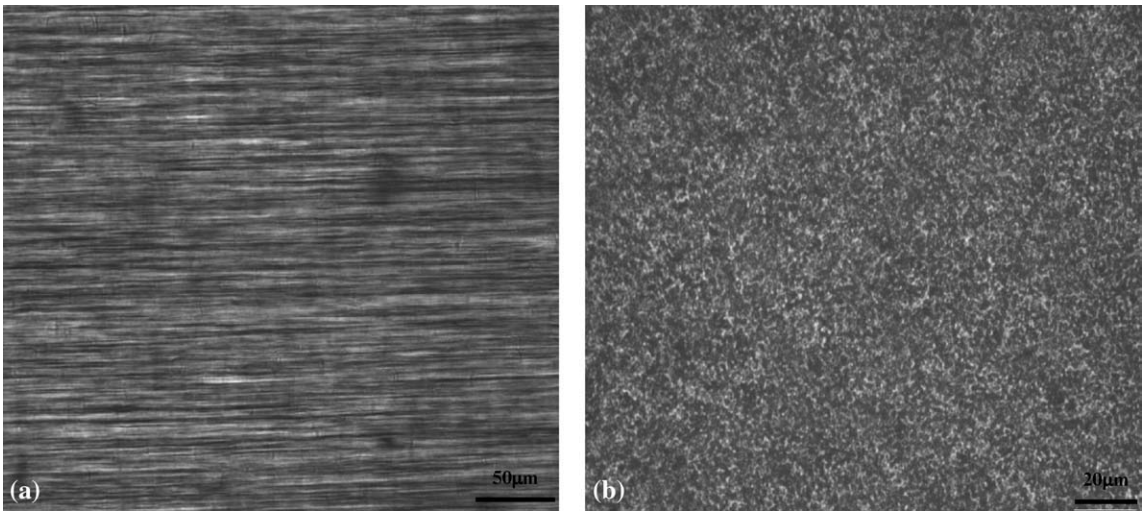

Fig. 2. Optical microscopy image of a PEMMA/γ-Fe_2O_3 film formed (**a**) under magnetic field, (**b**) without the application of the magnetic field.

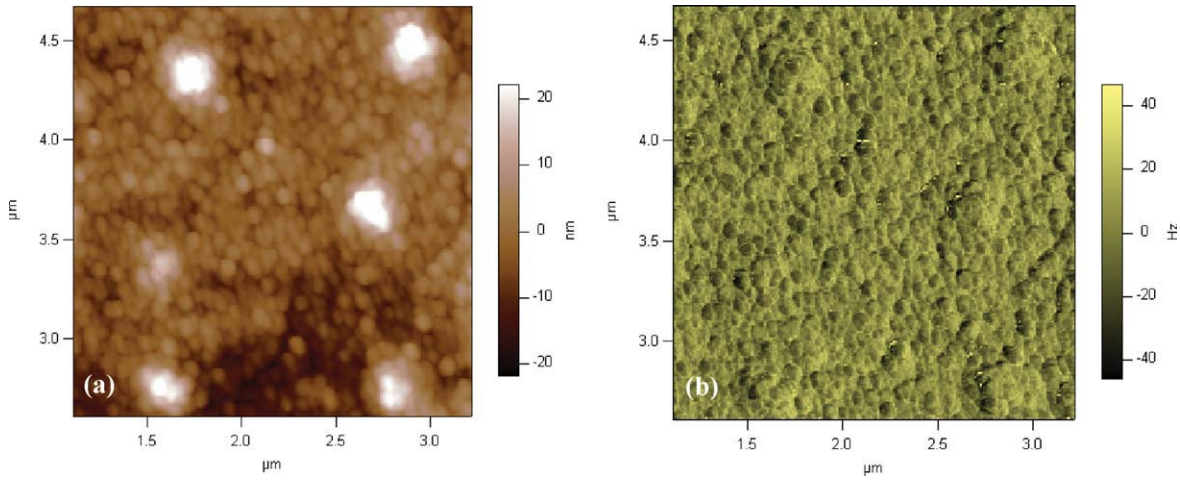

Fig. 3. **(a)** Topography and **(b)** magnetic field image of a film of 1% wt γ-Fe_2O_3 nanoparticles in PEMMA formed upon solvent evaporation of a drop-casted solution without the application of external MF.

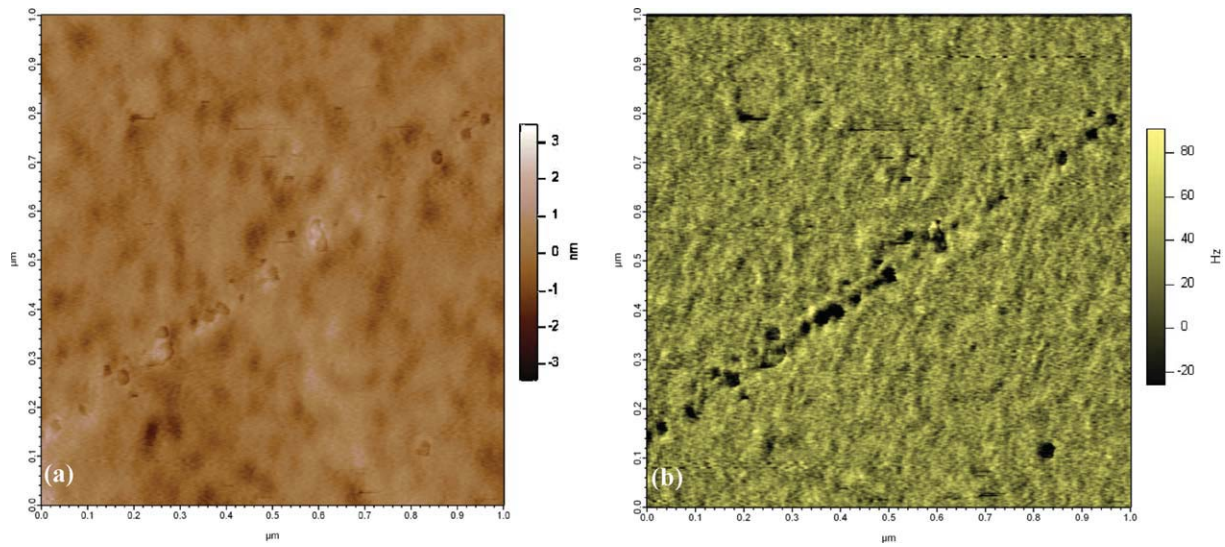

Fig. 4. **(a)** Topography and **(b)** magnetic field image of a film of 1% wt γ-Fe_2O_3 nanoparticles in PEMMA formed upon solvent evaporation of a drop casted solution under an external MF.

seen in Figures 4a and 4b, although, as mentioned earlier, the appearance of such features is not very frequent. Specifically, at the presented image is demonstrated a line with different magnetic behavior compared to the rest of the film, which is attributed to the magnetic nanoparticles assembly.

After the surface study of the films that gave very little information of the formation of the NWs upon MF application, slices of 200-nm thickness of the formed films were cut parallel to the MF lines, using an ultramicrotome. The MFM study was repeated on these slices, because, following this procedure, the surface layer was removed, and the examination was performed onto inner layers of the films. Specifically, Figure 5 shows the topography, the phase image, and the magnetic image of an $\sim 20 \times 20$-μm^2 area of a cut slice. The long-aligned NWs clearly appear throughout the surface of the section, and they exhibit enhanced magnetic properties, as the phase and magnetic images prove, respectively. The results verify the existence of long-magnetic NWs aligned throughout the volume of the films formed under the MF application that do not appear on the surface layers of the films and can only be monitored by MFM using ultramicrotomed film slices.

To examine further the formation of the NWs throughout the films and to specify in detail the composition of the nanocomposites, we performed TEM and SEM studies. The examination was done on slices cut from the films with the ultramicrotome. For the TEM analysis, the slicing of the pieces was done in directions longitudinal and vertical to the expected orientation of the NWs (Figs. 6a and 6b). The TEM images confirm

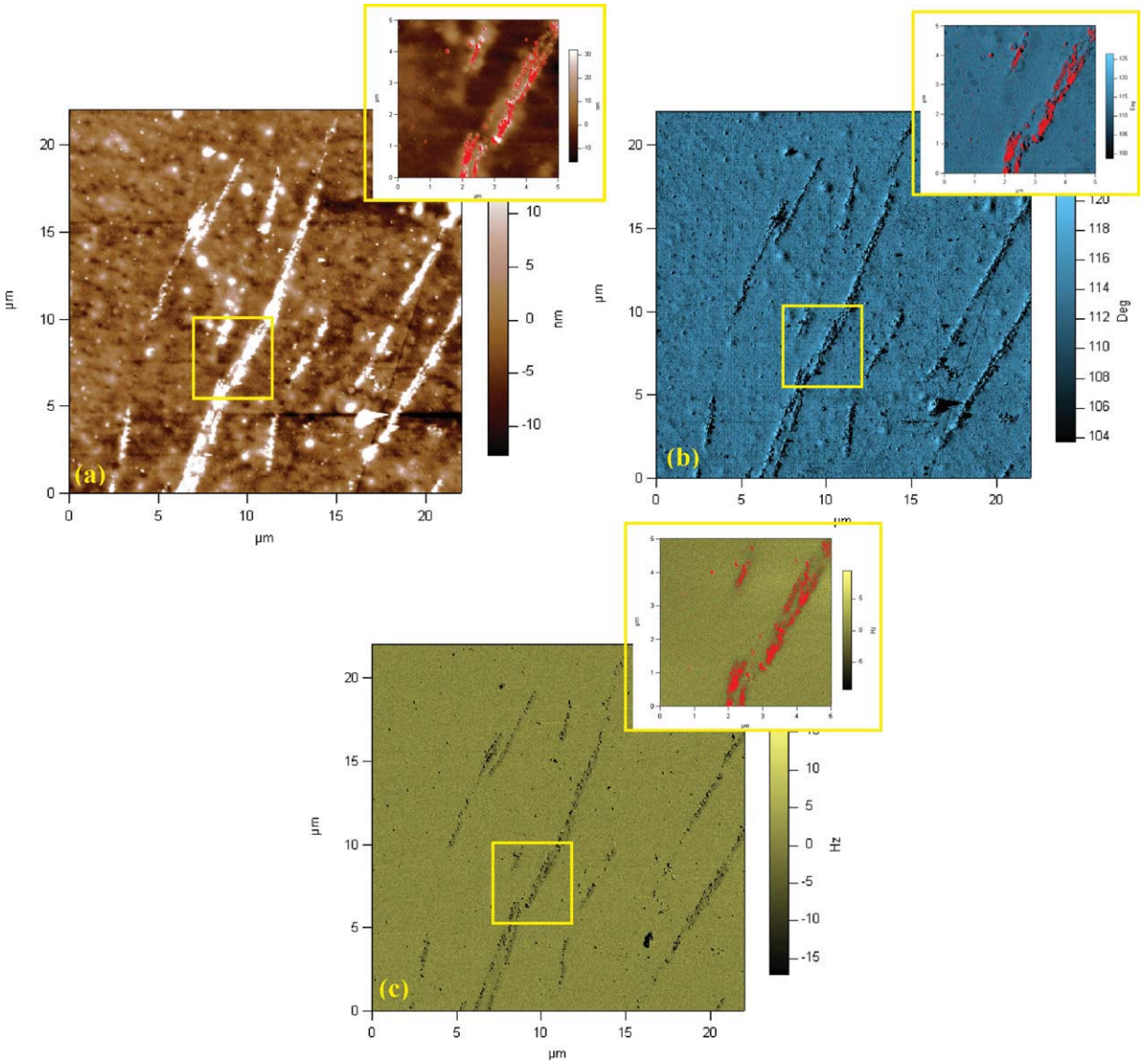

Fig. 5. **(a)** Topography, **(b)** phase image, and **(c)** magnetic image of a film slice of 200-nm thickness. The insets correspond to the area indicated with the yellow rectangular. The red mask used at all the insets indicates the threshold value for the total NAP signal. During NAP mode, the tip is lifted around 9 nm from the surface of the films.

the existence of NWs formed along the lines of MF, having cylindrical shapes, and being composed by aligned bundles of γ-Fe_2O_3 nanoparticles (Fig. 6).

A BSE–SEM cross sectional study on a slice cut parallel to the MF direction throughout the entire film shows that all the formed NWs follow the lines of the MF and that they are present in the whole film volume (Fig. 7a). The same study on a film formed without the application of MF shows that aggregates of γ-Fe_2O_3 nanoparticles are dispersed randomly throughout the volume of the nanocomposite film (Fig. 7c). An important observation is that the surfaces of the all films consist of a continuous layer of closely packed nanoparticles, independently from the application or not of the MF (Fig. 7b). We believe that this layer makes hard the observation of the formed NWs, during the topography characterization of our films using MFM, as mentioned previously.

DISCUSSION

The presented study demonstrates the possibility to create polymeric nanocomposite films incorporating unidirectional magnetic MWs. We demonstrate the detailed characterization of these films using a combination of different microscopic techniques that allows simultaneous locally selected topographic and magnetic measurements. The formation and alignment of the magnetic NWs occurred upon solvent evaporation of a drop-casted polymer/nanoparticles solution under the application of a MF. In detail, the static MF was applied on a solution of 1% wt γ-Fe_2O_3 colloidal nanoparticles and PEMMA in chloroform, drop casted onto

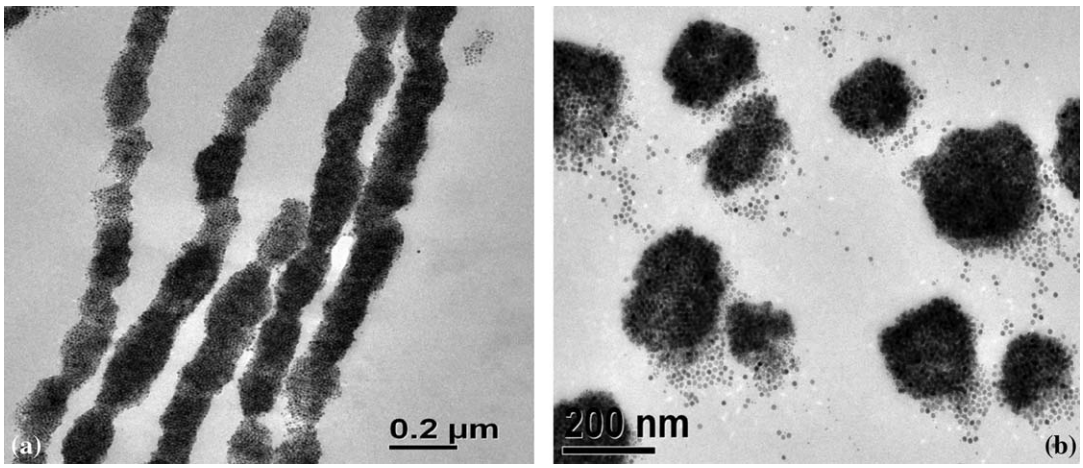

Fig. 6. **(a)** BF–TEM longitudinal image of a thin slice of a film (250 nm), where the NWs are shown parallel to their axis. **(b)** BF-TEM cross sectional image of a thin slice of the same film, showing the NWs perpendicular to their axis. Some dispersed particles apparent in this image are due to the cutting procedure.

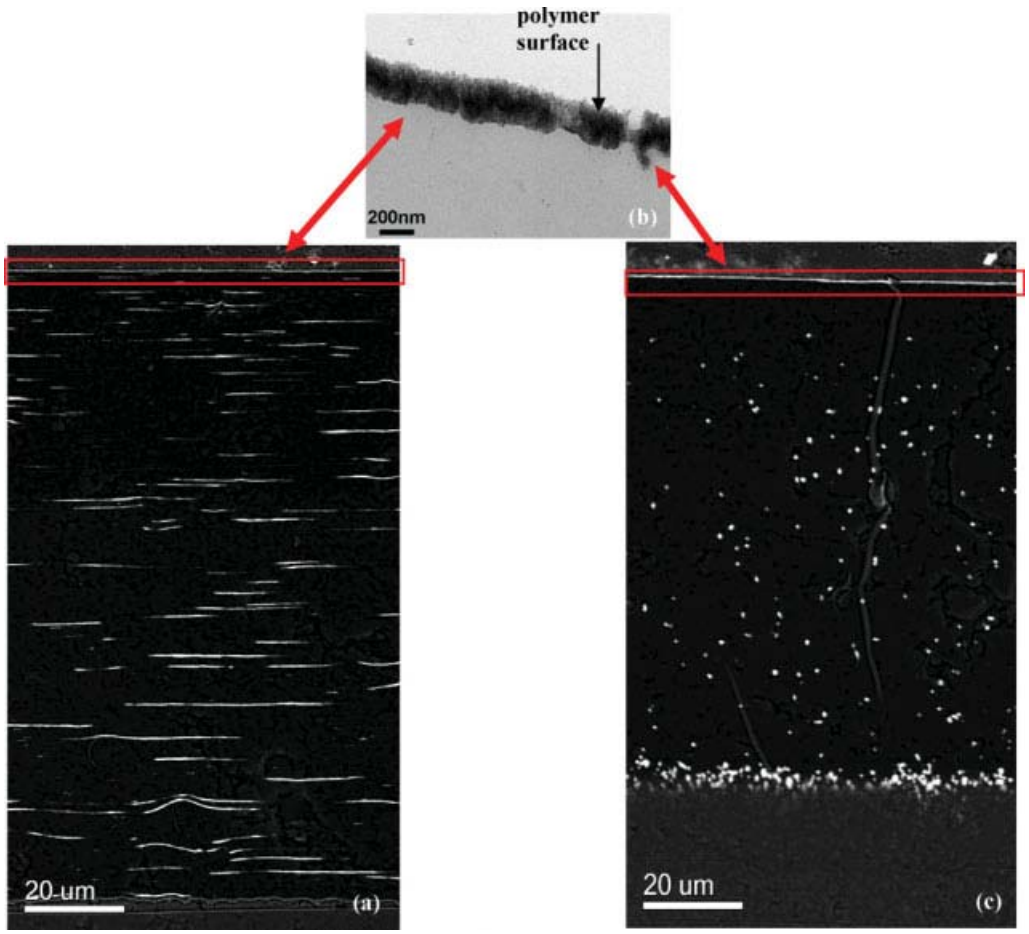

Fig. 7. **(a)** BSE–SEM cross sectional image of the whole film. The bright lines represent the NWs while the dark area is the polymer matrix. The bended NWs, observed at the lower part of the film, are due to the bending of the section. **(b)** BF–TEM image of the surface of the films, where a continuous layer of nanoparticles is observed. **(c)** BSE–SEM cross sectional image of the whole film formed after drying of a drop-casted solution without application of external magnetic field. [Color figure can be viewed in the online issue, which is available at wileyonlinelibrary.com.]

a glass substrate, at room temperature. The assembly of the nanoparticles is performed during the overnight solvent-evaporation process, following the direction of the lines of the MF. After the solvent evaporation, the obtained NWs remain eventually "frozen" in the solid film throughout its entire volume. Thus, a plastic film is formed incorporating well-aligned long NWs of average length ~15 μm and average diameter ~80 nm, as the SEM and TEM studies have shown. Additionally, the SEM study reveals that the surface layers of all the formed films are covered with closely packed γ-Fe_2O_3 nanoparticles distributed all over the surface not following the MF lines, even if the volume of these films contains aligned NWs. The formation of this layer can be attributed to the evaporation process. In particular, the very first seconds after the drop-casting procedure, it is expected that the solvent evaporation occurs much faster on the top layer of the film than at the rest of the casted solution. Thus, immediately after the deposition of the nanocomposite solution, a layer is formed with very high viscosity on the liquid–air interface, obstructing the movement of the nanoparticles and, thus, resulting in their fast immobilization. At the rest of the film, the viscosity is lower, due to the slower evaporation process, allowing to the nanoparticles to move following the magnetic lines, when the MF is applied, eventually forming NWs in the volume of the films. Upon subsequent solvent evaporation, the viscosity of the film gradually increases, slowing down the motion of the nanoparticles/NWs. Eventually, when the solvent is completely evaporated from the film, the viscosity becomes high, so that the formed NWs can be considered stable, being unable to decompose back to the nanoparticles, even if the MF is removed.

The removal of the surface layer of the films made possible their simultaneous topographic and magnetic study. Using a microtome, thin slices from the films were examined, having the aligned NWs exposed onto their surface. On these slices, the morphology and the magnetic properties of each individual NW could be studied. The formed NWs exhibit enhanced magnetic contrast revealed by the MFM study, proving that the NWs preserve the magnetic character of their individual components (γ-Fe_2O_3 nanoparticles). The study of the properties of individual stripes opens up the possibility of various applications of these films, related to the oriented growth and patterning of molecules bound on the NWs and to the effect of this binding on the magnetic properties of the NWs. In particular, work is in progress in our laboratories concerning the binding of these stripes with various biological molecules such as DNA, proteins, or cells, and the study in the change of the magnetic properties of the stripes using the MFM technique. Applying this method, the use of plastic films in biological applications for the formation of biological sensors and molecular recognition devices becomes possible.

REFERENCES

Fahrni F, Prins MWJ, van Ijzendoorn LJ. 2009. Magnetization and actuation of polymeric microstructures with magnetic nanoparticles for application in microfluidics. J Magn Magn Mater 321:1843–1850.

Goubault C, Leal-Calderon F, Viovy J-L, Bibette J. 2005. Self-assembled magnetic nanowires made irreversible by polymer bridging. Langmuir 21:3725–3729.

Huo J, Wang L, Yu H. 2009. Polymeric nanocomposites for electromagnetic wave absorption. J Mater Sci 44:3917–3927.

Jestin J, Cousin F, Dubois I, Ménager C, Schweins R, Oberdisse J, Boué F. 2008. Anisotropic reinforcement of nanocomposites tuned by magnetic orientation of the filler network. Adv Mater 20:2533–2540.

Kaushik A, Solanki PR, Ansaria AA, Sumanaa G, Ahmadb S, Malhotraa BD. 2009. Iron oxide-chitosan nanobiocomposite for urea sensor. Sens Actuators B 138:572–580.

Kimura T, Ago H, Tobita M, Ohshima S, Kyotani M, Yumura M. 2002. Polymer composites of carbon nanotubes aligned by a magnetic field. Adv Mater 14:1380–1383.

Lalatonne Y, Motte L, Russier V, Ngo AT, Bonville T, Pileni MP. 2004. Mesoscopic structures of nanocrystals: Collective magnetic properties due to the alignment of nanocrystals. J Phys Chem B 108:1848–1854.

Marti Y, Williams CC, Wickramasinghe HK. 1987. Atomic force microscope–force mapping and profiling on a sub 100-Å scale. J Appl Phys 61:4723–4729.

Martin J, Mijangos C. 2009. Tailored polymer-based nanofibers and nanotubes by means of different infiltration methods into alumina nanopores. Langmuir 25:1181–1187.

Martin JE, Venturini E, Odinek J, Anderson RA. 2000. Anisotropic magnetism in field-structured composites. Phys Rev E 61:2818–2830.

Merkel TC, Freeman BD, Spontak RJ, He Z, Pinnau I, Meakin P, Hill AJ. 2002. Ultrapermeable, reverse-selective nanocomposite membranes. Science 296:519–522.

Park J I, Jun Y W, Choi J S, Cheon J. 2007. Highly crystalline anisotropic superstructures via magnetic field induced nanoparticle assembly. Chem Commun 5001–5003.

Sahoo Y, Cheon M, Wang S, Luo H, Furlani EP, Prasad PN. 2004. Field-directed self-assembly of magnetic nanoparticles. J Phys Chem B 108:3380–3383.

Schmidt G, Malwitz MM. 2003. Properties of polymer–nanoparticle composites. Curr Opin Colloid Interf Sci 8:103–108.

Singh H, Laibinis PE, Hatton AT. 2005. Synthesis of flexible magnetic nanowires of permanently linked core-shell magnetic beads tethered to a glass surface patterned by microcontact printing. Nano Letters 5:2149–2154.

Sun S, Zeng H, Robinson DB, Raoux S, Rice PM, Wang SX, Li G. 2004. Monodisperse MFe_2O_4 (M = Fe, Co, Mn) Nanoparticles. J Am Chem Soc 126:273–279.

Tang Z, Kotov NA. 2005. One-dimensional assembly of nanopartilcles: preparation, properties and promise. Adv Mater 17:951–962.

Weller D, Doerner MF. 2000. Extremely high-density longitudinal magnetic recording media. Annu Rev Mater Sci 30:611–644.